IEEE Journal of Translational Engineering in Health and Medicine

Received 5 October 2022; revised 14 March 2023; accepted 26 April 2023.
Date of publication 3 May 2023; date of current version 10 May 2023.

Digital Object Identifier 10.1109/JTEHM.2023.3272796

Parkinson's Disease Diagnosis With Gait Characteristics Extracted Using Wavelet Transforms

DIXON VIMALAJEEWA, ETHAN MCDONALD, MEGAN TUNG, AND BRANI VIDAKOVIC

Department of Statistics, Texas A&M University, College Station, TX 77843, USA

CORRESPONDING AUTHOR: D. VIMALAJEEWA (dixon.vimalajeewa@tamu.edu)

This work was supported by Herman Otto Hartley endowed chair funds at Texas A&M University.

ABSTRACT Objective: Parkinson's disease (PD) is a common neurodegenerative disorder among adult men and women. The analysis of abnormal gait patterns is among the most important techniques used in the early diagnosis of PD. The overall aim of this study is to identify PD patients using vertical ground reaction force (VGRF) data produced from subjects while walking at a normal pace. Methods and procedures: The current study proposes a novel set of features extracted on the basis of self-similar, correlation, and entropy properties that are characterized by multiscale features of VGRF data in the wavelet-domain. Five discriminatory features have been proposed. PD diagnosis performance of those features are investigated by using a publicly available VGRF dataset (93 controls and 73 cases) and standard classifiers. Logistic regression (LR), support vector machine (SVM) and k-nearest neighbor (KNN) are used for the performance evaluation. Results: The SVM classifier outperformed the LR and KNN classifiers with an average accuracy of 88.89%, sensitivity of 89%, and specificity of 88%. The integration of these five features from the wavelet domain of data, with three time domain features, stance time, swing time and maximum force strike at toe improved the PD diagnosis performance (approximately by 10%), which outperforms existing studies that are based on the same data set. Conclusion: with the previously published approaches, the proposed prediction methodology consisting of the multiscale features in combination with the time domain features shows better performance with fewer features, compared to the existing PD diagnostic techniques. Clinical impact: The findings suggest that the proposed diagnostic method involving multiscale (wavelet) features can improve the efficacy of PD diagnosis.

INDEX TERMS Wavelet transform, self-similarity, entropy, level-wise cross correlation, classification, Parkinson's disease.

I. INTRODUCTION

Parkinson's Disease (PD) is the second most common neurodegenerative disease after Alzheimer's disease. Population prevalence of PD increases from about 1 percent at age 60 to 4 percent by age 80 [1]. PD primarily affects the motor regions of the central nervous system, causing abnormalities in gait (unintended or uncontrollable movements), such as shaking, stiffness, and difficulty with balance and coordination [2]. Over time, simple movements become more and more difficult for patients. The most evident benefit of early intervention is a reduction in symptoms, particularly dyskinesia, and the delay of levodopa initiation [3]. PD is clinically diagnosed based on medical history or through neurological examination [4]. The reliable diagnosis of PD using these tests is very difficult and prone to error, especially in the early stages [5]. There is high demand for more advanced PD diagnosing techniques.

Several bodily functions in individuals with PD are affected and have been used in developing advanced PD diagnostic techniques. One of the most commonly monitored functions is gait, as PD has major effects on the central motor system. Gait abnormalities have been measured through vertical ground reaction force (VGRF) data collected from pressure sensors placed on the bottom of shoes while individuals walk [6]. Additionally, other measurements such as speech abnormalities and reactions to emotional states

have also been useful in PD diagnosis, as reported by Zhang et al. [7] and Ali et al. [8], and Murugappan et al. [9]. Based on these body functions, multiple computer-aided methods have been proposed for automated PD detection. Readers can find more information about these automated technologies in Mughal et al. [10].

The majority of published methods focus on feature extraction either in the domain of data acquisition (i.e., time-domain), frequency/scale domain, or time-frequency/scale domain. For instance, Alam et al. [11] investigated different time domain features such as swing time, stride time variability, and center of pressure and also procedures to select the most meaningful of these features for PD diagnosis. The forward feature selection procedure with support vector machine classifier outperformed other classifiers with an accuracy of 93.6%. This study, however, used only a small VGRF dataset (29 cases and 18 controls) published by Yogev et al. [12]. By using a larger VGRF dataset, Lee et al. [13] proposed a neural network and weighted fuzzy membership based model, and achieved classification accuracy of 77.33%. Gait asymmetry features, such as step time, stance time, and double stance time, were introduced via a time-frequency analysis on VGRF data in Su et al. [14]. The study reported that the degree of asymmetry of the proposed features in PD patients is higher than in the control subjects. The main advantage of these methods is that physicians and scientists can use insights associated with selected features to further understand the nature of PD and take a confident action in clinically diagnosing the disease.

As reflected by a vibrant research, wavelets are standard signal processing tools useful in developing effective feature extraction procedures for analyzing high frequency and noisy signals. Wavelets decompose a signal into a set of coefficients belonging to different scales, and the analysis of these coefficients can produce valuable information that can be used in disease diagnosis [15]. In recent studies, wavelet-based features have been extracted from movement-related signals such as VGRF and used to distinguish PD patients from healthy controls. For instance, Su et al. [14] used wavelet transform to compute gait correlation at different frequency sub-bands to characterize gait symmetry between the left and right legs. Those correlations were then used to differentiate PD patients from control subjects. Also, Murugappan et al. [9] proposed a wavelet-based approach to characterize variability in emotions of PD patients. However, the majority of studies have used wavelet primarily as a data pre-processing technique for constructing complex PD diagnosis models [13], [16]. Those studies did not take into account potentially valuable information in gait time series, such as fractality, self-similarity, and long-memory, that could be effectively assessed through wavelet transforms and that have demonstrated significant discriminatory power, especially in the medical context [17], [18], [19]. Thus, to the best of our knowledge, there are no studies that have accounted for the full potential of wavelets, especially in feature extraction, in the context of PD diagnosis. In the context of diagnosing PD, this study first uses the range of multiscaling features in gait data derived in the wavelet domain.

In summary, the current study proposes a novel set of discriminatory features in the VGRF data. The gait properties which are explored in the wavelet domain include self-similarity, level-wise cross correlations, and level-wise entropies. Self-similarity is a property of a signal to exhibit similar characteristics when inspected at different resolutions. This property primarily allows for characterizing regularity of gait signals. Level-wise cross correlations explore relationships that may exist in gait data at different scales compared to the standard correlation that is used frequently in the time domain of data. The measure of compressibility (coding complexity) in gait data is characterized by wavelet entropy. In total, nine multiscale (wavelets-based) features were derived by using these three properties. The forward feature selection procedure was used to select most significant features. We explored their potential in distinguishing gait patterns between PD patients and control subjects by using logistic regression (LR), support vector machine (SVM), and k-nearest neighbor (KNN) classifiers on a publicly available VGRF dataset. PD diagnosis performance was further investigated by combining the selected five multiscale features with three time domain features, namely stance time, swing time and maximum force strike at the toe. The obtained results showed the positive effect that this feature set could have on an enhanced PD diagnosing performance compared to the previously published studies that used the same VGRF dataset.

The remainder of the paper is organized as follows. Details of the VGRF dataset and feature extraction methods are discussed in Section II. Methodology is described in Section III, followed by Section IV, which describes the data analysis procedure. Section V presents the performance of the proposed feature set. Discussion and Conclusions are provided in Sections VI and VII, while the technical details and additional results are provided in Appendices A-E.

II. DATASET

The data used in this study is published at *Physionet.org*. It contains measures of gait from 93 PD patients (mean age: 66.3 years; 63 percent men), and 73 controls (mean age: 66.3 years; 55 percent men) collected in three independent studies [12], [20], [21]. These three studies followed similar protocols and had the same data acquisition devices. Underneath each foot, eight force sensitive insole sensors were placed evenly dispersed between the heel and the toe, and they each produced their own results. The vertical ground reaction force measurements from the subjects were obtained at 100Hz as they walked at their normal pace for 2 minutes on a flat surface. Figure 1 shows a sample VGRF data of a case and control subject for 10 seconds. A detailed description of the dataset can be found in Hausdorff [22], while a description of the insole sensors can be found on the manufacturer's website *Ultraflex Computer Dyno Graphy, Infotronic Inc's* [23].

IEEE Journal of Translational Engineering in Health and Medicine

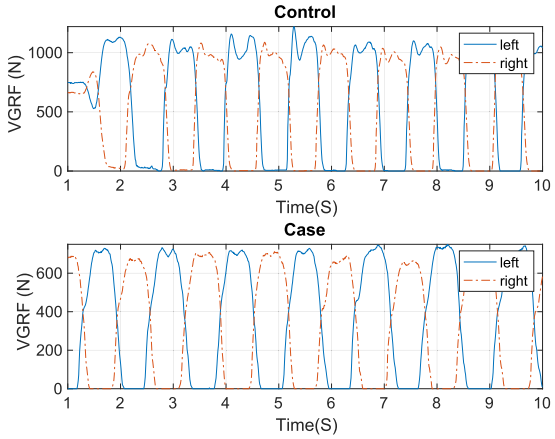

FIGURE 1. A sample vertical ground reaction force (VGRF) signal during walking. Ten seconds of a VGRF signal of the left and right leg from a randomly selected PD patient and control subject.

1) DATA PRE-PROCESSING

According to the experimental settings used in data collection process (VGRF measures for 2 minutes at 100 Hz), there should be 12,000 data points per signal. In some cases, however, the number of data points present in data files varies significantly. More precisely, the number of observations per person in the case group ranges from 4,363 to 26,366, while in the control group, it ranges from 4,034 to 12,119. We selected individuals whose VGRF signals contain at least 8,192 (2^{13}) data points to make subsequent discrete wavelet transforms simple. As a result, 86 PD subjects from the case group and 63 subjects from the control group were selected.

During the process of extracting time domain features, we encountered small sensor readings during the stance phase, which is unexpected as this phase is generally considered not to produce any ground reaction force. We treated these values as noise and set VGRF readings below 20 N to zero.

III. METHODOLOGY

A. FEATURE EXTRACTION

In the current study, the feature extraction procedure relies mainly on the scale/frequency domain, specifically, on the features derived from the VGRF data in the wavelet-domain. In the following, an overview of the wavelet transform procedure is provided prior to describing features extracted through wavelet transforms. This is followed by the description of commonly used time domain features.

B. WAVELET TRANSFORMS-BASED FEATURES

1) WAVELET TRANSFORMS

Wavelet transforms (WTs) are a standard tool in signal processing and are commonly used for analyzing a high frequency signals. WTs, as scale-time decompositions, are defined in terms of a scale, a parameter that determines the support of wavelet basis function, and a shift parameter that determines wavelet location in the time domain. The scales are discrete, ranging over dyadic values, that is, each coarser scale in the wavelet representation is twice the size of the finer one. The frequency is a reciprocal of scale, and as the scales are discrete, the frequencies in wavelet representation are discrete as well. The finest (smallest) scale corresponds to the Nyquist frequency in wavelets and for each subsequent larger scale, the frequency is two times smaller.

The application of the WT on a data signal results in a decomposition of the signal into a set of contributions that are localized both in the time and scale. More precisely, wavelets decompose a signal into a hierarchy of resolutions convenient for the extraction of various scale-sensitive descriptors. For example, such descriptors can be linked to the presence of long memory, fractality, and self-similarity, as well as the correlations and entropies confined to a particular scale.

Discrete wavelet transforms (DWTs) are a popular version of WTs applicable to discrete data, such as sampled signals. Technical details about DWT can be found in Appendix A. Analysis of the resulting coefficients from DWT allows for the extraction of valuable insights that could be useful in understanding and characterizing underlying behaviors of the signal. In the following, we extract three important descriptors of the VGRF signals in the wavelet-domain, to define discriminatory descriptors.

For the extraction of wavelet-based features described below, we used the minimal phase Daubechies 6 wavelet (3 vanishing moments, 6 tap filter). This filter is a compromise between the locality of representation and the smoothness of decomposing scaling function. The two more local filters Daubechies 2 (Haar) and Daubechies 4 are not smooth, while Daubechies 6 is the most compact wavelet for which the scaling function is differentiable [15]. Moreover, frequency is the reciprocal of scale, and in this study, the original VGRF time series had a sampling rate of 100 Hz. The finest scale, which represents the smallest detail, corresponds to a Nyquist frequency of 50 Hz. The wavelet coefficients are distributed across different scale levels, denoted by 12, 11, 10, and so on, in log base 2 units of the number of coefficients in that level. The corresponding frequencies for these scales are 50 Hz, 25 Hz, 12.5 Hz, 6.25 Hz, and so on. Since scales are discrete, the frequencies are also discrete, and each scale corresponds to a specific frequency that is a dyadic ratio of the sampling frequency. It is important to note that a specific scale does not correspond to a range of frequencies, but to a single frequency that is determined by the dyadic ratio.

2) SPECTRAL SLOPE

Self-similarity is an omnipresent phenomenon that characterizes high frequency time series obtained in different contexts: health, geoscience, economics, and physics, to list a few. This behavior refers to the stochastic similarity in a signal when viewed at different scales. In the wavelet domain, self-similarity is quantified commonly by using the wavelet spectra. The wavelet spectrum of a signal consists of wavelet log-energies (logarithm of average squared wavelet

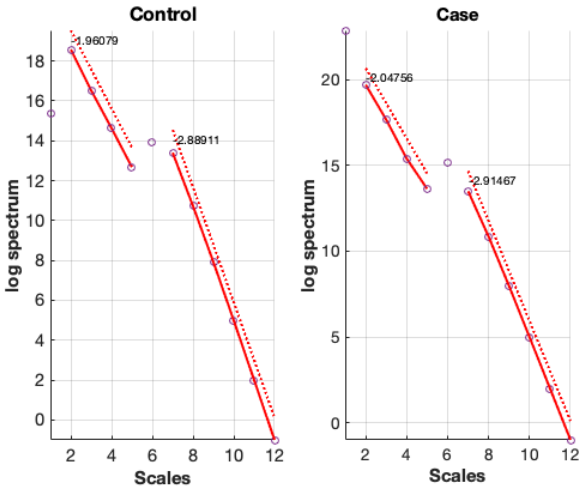

FIGURE 2. Sample wavelet spectra for the case and control group. Wavelet spectra computed using a VGRF signal of the right leg are shown in 1. The coordinate of the point at the scale index (or level) j is $\log_2(\bar{d}_j^2$ (aka log energy of wavelet coefficients d at level j), where $\bar{d}_j^2$ is the average-square of the wavelet coefficients at the wavelet decomposition level j (see Appendix A for more details on wavelet coefficients d). Slope-1 and slope-2 of the wavelet spectra are estimated by fitting a straight line (green dashed) on the log energy of the wavelet coefficients (black circles) within the scale index j ranging from 2 to 5 and from 7 to 12 (red line).

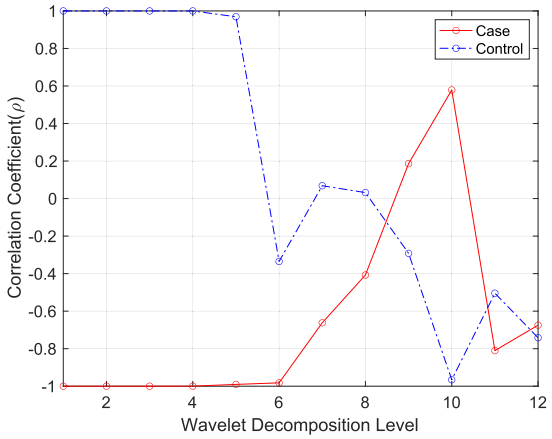

FIGURE 3. Sample level-wise cross correlation coefficient for case and control group. The level-wise cross correlation coefficients show breakdown of the typical sample correlation into a weighted sum of correlations of the VGRF signals shown in Figure 1. This breakdown provides a detailed examination of the correlation structure between two aligned VGRF time series corresponding to the left and right leg, making it possible to identify linear relationships at more precise scales, corresponding to various frequency bands that are finer than the VGRF values sampled.

coefficients) as a function of resolution level. Technical details about wavelet spectra are given in Appendix B.

In general, it is accepted that a given signal possesses the self-similar property if its wavelet spectrum exhibits a regular decay with an increase of resolution scales. The rate of the log energy decay (slope) is connected with the Hurst exponent ($H \in [0, 1]$), which characterizes the regularity of the signal. To estimate the slope, the linear regression of log energies to the scale index is found and then H is computed as $H = -(slope + 1)/2$. The spectral slope theoretically ranges from -3 to -1. Larger slopes (> -2) indicate a higher degree of persistence (i.e., more regular/smooth signal), and smaller slopes (< -2) indicate a higher degree anti persistency and intermittency. The Hurst exponent serves as a measure of signal regularity. Signals with a Hurst exponent close to 1 are more regular (smooth), while the signals with a small Hurst exponent are highly irregular. Overall, the degree of regularity expressed by either spectral slope, or equivalently by the Hurst exponent, represents an informative summary of a complex and noisy signal for which standard statistical summaries (moments, trends, etc) may be irrelevant.

Self-similarity is one of the behaviors of interest in the VGRF time series. As evident from previous studies [19] and [24], the self-similar property in high frequency signals and images has been explored frequently in the wavelet domain for different medical diagnosis purposes. In those studies, slope of the wavelet spectra is one of the commonly used discriminatory features. The present study also explores the self-similar nature of VGRF time series for distinguishing gait dynamics of PD patients from that of control subjects.

As can be seen in Figure 2, the wavelet spectra of a VGRF time series exhibit a self-similar property. However, when inspected closely, the log energies among scale indexes 2-5 and 7-12 decay with different slopes. This is due to the fact that the energies below the sixth scale index reflect the gait dynamics between steps, while the energies above the sixth scale index correspond to the gait dynamics within the steps. Consequently, slope-1 and slope-2 are computed for the range of scales 2-5 and 7-12, respectively, excluding the log energy at the sixth scale. We use slope-1 and slope-2 as two discriminatory features in distinguishing gaits between PD patients and controls. It is important to note that if the features correspond to frequencies higher than the frequency of walking, we termed those as "between steps" features. If the frequency attributes (corresponding to a scale of a selected feature) are higher than the frequency of walking steps, then we termed those as "within steps".

3) LEVEL-WISE CROSS CORRELATION

Level-wise cross correlation assesses the correlation between two signals at various resolutions (scales). This enables us to explore the individual contribution of correlations at each of the scales to the sample correlation between those two signals in the original data domain. That is, in the wavelet domain, the sample correlation can be expressed as the weighted sum of the level-wise cross correlation coefficients, which are the correlations between the corresponding wavelet coefficients of the two signals at matched scales. Thus, due to orthogonality of wavelet transforms, the level-wise cross correlations can be related effectively to the correlations in the original data domain, providing additional information about nature of relationships that may exist at a particular scale(s). More specifically, the level-wise correlation enables

IEEE Journal of Translational Engineering in Health and Medicine

TABLE 1. The set of multiscale (wavelet transforms-based) and time domain features considered in the present study.

Feature	Name	Description
Multiscale(wavelet transforms-based) Features		
1-6	Level-wise cross correlation	Cross correlation coefficient of detail wavelet coefficients of VGRF time series correlation coefficients between left and right leg with six wavelet decomposition levels computed by using Eq 6 in Appendix C.
7	Slope-1	Average spectral slope between scale index 2-5 of eight sensors computed by using Eq 3 in Appendix B.
8	Slope-2	Average spectral slope between scale index 7-12 of eight sensors computed by using Eq 3 in Appendix B.
9	Wavelet Entropy	Non-normalized Shannon entropy of wavelet coefficients at the 4th wavelet decomposition level by using Eq 7 in Appendix D.
time domain Features		
1	Stance time	Average stance time of total VGRF of eight sensors.
2	Swing time	Average swing time of total VGRF of eight sensors.
3	Peak force at toe	Mean peak force at toe off.

capturing linear relationships at finer scales (at various frequency bands 50 Hz, 25 Hz, 12.5 Hz and so on) than at which VGRF values have been sampled.

Due to walking disorders in PD patients, their gait correlations between left and right leg could be significantly different from those in control subjects. The sample correlation between two aligned VGRF time series, corresponding to the left and right leg, gives only a general overview about such relationships. The analysis of such relationships using the level-wise cross correlation results in a set of correlations and subsequently has more potential to identify abnormal gait dynamics, that be influenced by correlations at particular scale. For instance, as can be seen in Figure 3, the level-wise cross correlation coefficients of gaits in PD patients and control subjects are clearly distinguishable over the first six wavelet decomposition levels. Hence, those level-wise cross correlation coefficients are used as another set of discriminatory features. To extract cross correlation features, we specifically choose wavelet decomposition level 6 to split scales in the wavelet domain. This is based on the observation that cross correlations above level 6 did not exhibit a notable difference between cases and controls. Readers can find more technical information about computing level-wise cross correlation coefficients in Appendix C.

4) WAVELET ENTROPY

Wavelet entropy (WE) is frequently used as a natural measure of compressibility or complexity of signals. A signal generated from a random process can be considered as more or less complex, depending on the mechanism of the random generation. For example, if the signal is generated as a Gaussian iid process, the entropy is maximum among all random generation mechanisms with fixed mean and finite variance and the signal is not readily compressible. Moreover, standard Gaussian signal in the time domain corresponds to standard Gaussian signal in the wavelet domain and all level-wise wavelet entropies are theoretically the same. However, if the generating mechanism of a signal is not Gaussian, the level-wise entropies in its wavelet representation can be informative. In extreme cases, for example, an ordered signal (e.g., sinusoidal signal) exhibits a narrow peak in the wavelet domain which results in low entropy. More details about wavelet entropy of signals can be found in [25].

As reported in previous research [13] and [26], gait dynamics of healthy individuals have higher entropy compared to the individuals with PD. That is, a VGRF time series of a control subject exhibits more complexity, compared to a PD patient. More specifically, there is a significant difference in the level of synchrony between the two legs while walking comparatively between PD patients and controls. Therefore, wavelet entropy, in the present study, is used as a discriminatory feature to differentiate PD patients and controls. The unnormalized Shannon entropy of detail wavelet coefficients of a VGRF time series at the sixth wavelet decomposition level was selected. See Appendix C for more technical details about computing WE.

C. TIME DOMAIN FEATURES

As evident from previous studies, several time domain features that are based on VGRF time series data have been proposed for diagnosing PD. In general, they rely mostly on gait cycle dynamics. In the present study, two types of frequently used time domain features are listed below. These features have been found to be some of the most promising and frequently used ones for distinguishing gait dynamics between case and control subjects according to several previous studies [11], [27], [28], [29], [30], [30], [31], [32].

- **Swing time and stance time:** A gait cycle is made up of two phases: stance time and swing time. During the stance time phase, one leg is in contact with the ground. In contrast, during the swing time phase, the leg is not touching the ground. The duration and effort required to complete these two phases can vary, particularly in individuals with walking disorders. For example, people with Parkinson's Disease (PD) often exhibit increased variability in both stance and swing times compared to healthy individuals. In this study, we used the average stance and swing times of each participant as two time-domain features.
- **Peak force at toe off:** Patients with Parkinson's Disease (PD) often apply less pressure during the heel strike and toe-off phases of walking compared to healthy individuals. As a result, the maximum VGRF at heel strike

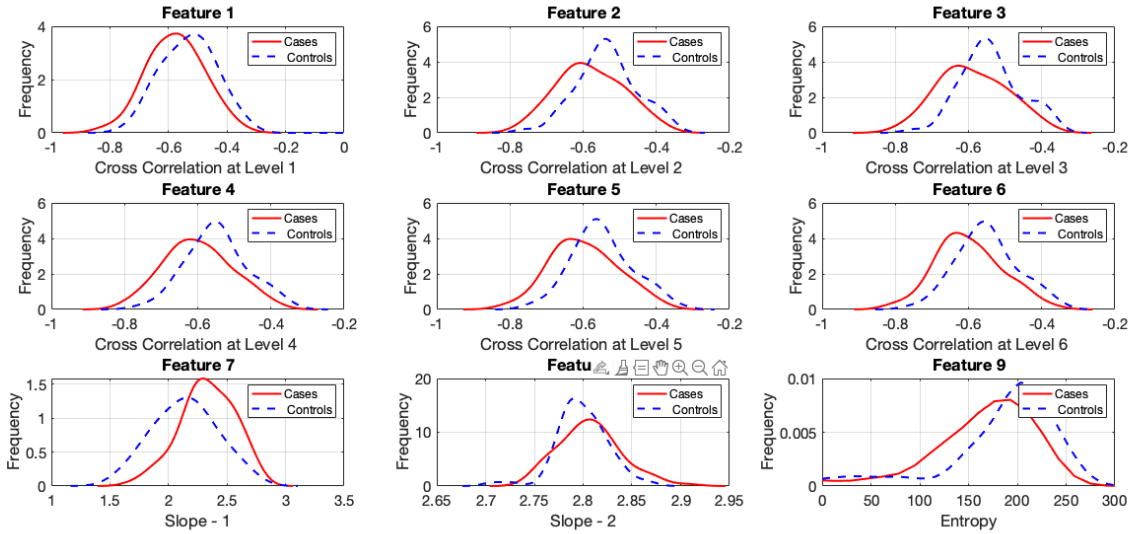

FIGURE 4. The distribution of nine multiscale features summarized in Table 1.

TABLE 2. The set of optimal multiscale features selected using forward feature selection method.

Classifier	Name	Feature
Logistic Regression (LR)	Level-wise cross correlation	4
	Slope-1 Slope-2	7 and 8
	Wavelet entropy	9
Support Vector Machine (SVM)	Level-wise cross correlation	4
	Slope-2	8
	Wavelet entropy	9
K Nearest Neighbor (KNN)	Level-wise cross correlation	4
	Slope-1 and Slope-2	7 and 8
	Wavelet entropy	9

TABLE 3. Comparison of different classifier performance (*mean* ± *std*) with the selected set of optimal multiscale features listed in Table 2.

Classifier	Classification Accuracy	Sensitivity	Specificity
Logistic Regression (LR)	83.27 ± 5.00	0.82 ± 0.01	0.84 ± 0.09
Support Vector Machine (SVM)	**88.89 ± 6.36**	**0.89 ± 0.08**	**0.88 ± 0.08**
K Nearest Neighbor (KNN)	86.15 ± 6.44	0.88 ± 0.05	0.84 ± 0.09

and toe-off can vary between PD patients and control subjects. In this study, we used the mean maximum toe-off force as a discriminatory feature.

IV. DATA ANALYSIS

We computed multiscale features, including slope, cross-correlation, and entropy, as well as time-domain features for either the left or right leg. These features were calculated for all eight sensors and then averaged. To compute the multiscale features, we used the cumulative sum of the z-scored vertical ground reaction force (VGRF) time series. For the time-domain features, we used the total sum of VGRF data from all eight sensors. This resulted in a set of nine multiscale features and three time-domain features, which are summarized in Table 1. Below, we describe the procedure used to evaluate the performance of these features in diagnosing Parkinson's Disease (PD).

A. CLASSIFICATION MODELS

Our data analysis involved evaluating three commonly used classification algorithms: Logistic Regression (LR), Support Vector Machine (SVM), and k-Nearest Neighbors (KNN). We used default model parameters in the context of analyzing vertical ground reaction force (VGRF) data. The LR classifier was implemented using stochastic gradient descent as the solver, while the SVM classifier used a linear kernel with automatic kernel scaling. The KNN classifier was based on the Euclidean distance metric and used five nearest neighbors for classification. To determine the optimal number of features for each model, we employed the sequential forward feature selection method.

B. FEATURE SELECTION

We used the sequential forward selection method to select features. This method involves selecting features one at a time based on a custom criterion that measures the performance of a learning algorithm, in this case, classification. The process involves creating candidate feature subsets by adding each unselected feature one at a time. We then performed 10-fold cross-validation on each candidate feature subset and calculated the average misclassification rate as the custom criterion to evaluate the performance of each subset.

After computing the mean misclassification rate values for each candidate feature subset, the sequential forward selection method selects the candidate feature subset that minimizes the average misclassification rate. This process continues until including additional features no

IEEE Journal of Translational Engineering in Health and Medicine

longer reduces the criterion. In our study, we used the default settings of the *sequentialfs* Matlab function and a more detailed explanation of this method can be found in [33].

C. PERFORMANCE EVALUATION

To fit the classification model, we randomly assigned 80% of the rows from each feature matrix to the training set and used the remaining rows for testing. To balance the group sizes for model training and testing, we randomly selected 63 subjects from the 86 Parkinson's Disease cases to match the number of controls. This was done to avoid bias due to imbalanced group sizes. We assessed classifier performance using sensitivity, specificity, and overall accuracy.

We repeated the data splitting and model performance evaluation process 100 times with the optimal feature subset for each classifier. The reported performance measures were averaged over these repetitions.

V. RESULTS

This section presents the performance of multiscale features and their combined use with time-domain features in distinguishing Parkinson's Disease (PD) patients from healthy controls. First, we discuss the selection of a subset of multiscale features for each classifier that contributes to achieving the highest classification performance using the forward feature selection procedure. Next, we integrate the selected subset of multiscale features with time-domain features and evaluate classifier performance using the combined feature set. In these analyses, we repeated the classifier performance evaluation 100 times and reported the average performance. We used MATLAB R2021b software for our data analysis [34].

A. PERFORMANCE OF MULTISCALE FEATURES

The set of nine multiscale features listed in Table 1 was computed by using the pre-processed VGRF dataset described in section II. Figure 4 shows the distributions of these features for the case and control groups. Overall, all feature distributions exhibit varying levels of discrimination between the two groups. To assess quantitative differences in discriminatory behavior, we conducted a Wilcoxon rank-sum test to evaluate the ability of the proposed features to distinguish between cases and controls. The results indicate that the medians of most features show a significant difference between the two groups (with a $p-value < 0.05$), except for cross-correlation at levels 1 and 2 in the wavelet domain features. This analysis is exploratory and designed to identify candidate features for classification.

We performed the sequential forward feature selection procedure with each classifier to select the subset of multiscale features that achieves the best classification performance. We executed the procedure with all possible permutations of multiscale features. The best feature subsets for the Logistic Regression (LR), Support Vector Machine (SVM), and k-Nearest Neighbors (KNN) classifiers were {9, 7, 4, 8}, {4, 7, 8, 9}, and {9, 8, 4} for the LR, SVM, and KNN classifiers, respectively. Table 2 summarizes the selected optimal feature sets for each classifier.

TABLE 4. Classifier performance with the integration of five WT-based features and three time domain features.

Classifier	Classification Accuracy	Sensitivity	Specificity
Logistic Regression (LR)	92.84 ± 3.19	0.99 ± 0.03	0.95 ± 0.08
Support Vector Machine (SVM)	**97.43 ± 2.93**	**0.99 ± 0.02**	**0.95 ± 0.06**
K Nearest Neighbor (KNN)	93.63 ± 4.72	0.96 ± 0.05	0.92 ± 0.07

The classification was performed with the selected subset of features. Table 3 summarizes classification performance of the three classifiers. The SVM classifier achieved the highest performance, followed by LR and KNN classifiers.

B. PERFORMANCE WITH BOTH TIME AND WAVELET DOMAIN (MULTISCALE) FEATURES

The classifier performance was evaluated by using the multiscale feature subsets and three time domain features listed in Table 1. The introduction of time domain features increased the classifier performance (see Table 4). The SVM classifier achieved the highest performance with a 97.43 ± 2.93%, sensitivity 0.99 ± 0.02, and 0.95 ± 0.06 specificity. This is followed by the KNN and LR classifiers.

VI. DISCUSSION

In contrast with earlier studies that used WT mostly as a data pre-processing tool in PD diagnosis, the present study proposes a novel set of features that are solely based on WT. Therefore, the present study emphasizes the greater potential of WT serving as a feature extraction tool in PD diagnosis. Additionally, incorporating multiscale features in conjunction with time domain features enhances PD diagnosis performance, as shown in Table 5. That is because they are derived respectively in frequency and time domain, and hence theoretically, they should be independent. As evident in Figure 5 in Appendix E, the majority of WT-based and time domain features do not share strong correlations. Comparing our PD diagnosis performance with that of previous studies using the same VGRF dataset, our classification technique displays better or comparable performance with a simple model.

Table 5 compares the feature extraction domain, features, and performance of our proposed method with previous studies that used the same VGRF dataset. Lee et al. [13] reported an overall accuracy of 77.33% by utilizing 40 frequency-domain features extracted via wavelet transform on VGRF data. These features primarily comprise frequency distributions of wavelet coefficients and their variabilities. The model proposed by Channa et al. [16] also employed frequency domain features, but it shows superior accuracy with a smaller number of features compared to Lee et al. [13]. Meanwhile, Srivardhini et al. [30] present a NN model that

TABLE 5. Performance comparison with the existing studies that used the same dataset.

Study	Feature Category	Features	Number of Features	Classification Accuracy	Classifier
Lee et al. [13]	Frequency domain	Mean of the absolute values of the wavelet coefficients in each sub-band, Median of the wavelet coefficients in each sub-band, Average power of the wavelet coefficients in each sub-band, Standard deviation of the coefficients in each sub-band, Ratio of the absolute mean values of wavelet coefficients of adjacent sub-bands.	40	77.33	NN
Channa et al. [16]	Frequency domain	Wavelet energy, variance, and entropy and standard deviation and waveform length.	5	90.30	SVM
Srivardhini et al. [30]	Time domain	Normalized aggregated VGRF values for left and right legs, Stance, stride, and swing times for left and right legs, Initial and terminal forces for left and right legs, Statistical covariance of each feature for both legs, step distance, and asymmetry index of the left and right leg.	34	97.41	NN
Proposed Method	**Time domain and Frequency domain**	level-wise cross correlations, spectral slope, and wavelet entropy and swing and stance times, maximum force at toe off	**8**	**97.43**	**SVM**

utilizes time domain features and outperforms many previous studies. By incorporating both time and frequency domain features as proposed in our study, we can achieve better or comparable performance with a relatively simple model (in terms of the number of features). Therefore, the integrated use of discriminatory features from different domains can lead to developing better-performing classifiers with a relatively smaller number of features.

The improved performance of our methodology is primarily due to the unique selection of classifying features that have higher discriminatory power compared to the features proposed in the previously published studies. To the best of our knowledge, this is the first study that introduces the level-wise cross correlation coefficients to classify gait in PD diagnosis, although the standard correlation coefficient frequently appears as a discriminatory feature. As we pointed out, the use of level-wise cross correlation coefficients allows for a more detailed analysis of the correlation structure of gait dynamics than the standard correlation coefficient. This allows for the characterization of the similarity between the VGRF time series of the left and right legs during walking. The cross correlations of the VGRF time series in PD patients are generally higher than those in the control group (Figure 4), suggesting that PD patients rely more heavily on both legs during walking due to their increased risk of falls resulting from gait disturbances. Additionally, PD patients have a more regular signal and less erratic gait dynamics compared to healthy controls, as indicated by a higher slope under features 7 and 8 in Figure 4. This can be attributed to less disruption of long-memory correlations in gait dynamics caused by walking disorders. Furthermore, the entropy of gait behaviors in PD patients is comparatively smaller than in healthy controls (Figure 4), indicating reduced complexity in gait dynamics. Overall, these multiscale features can be used as important tools for detecting abnormalities in gait patterns and tracking the progression of conditions such as PD.

It is worth to note that there are some algorithms that show near perfect classification performance based on the same dataset. For instance, El Maachi et al. [35] proposed a deep neural network classifier and differentiated PD patients from controls with 98.7% accuracy. However, the overall computational cost of deep neural network-based approaches is generally higher than the LR, KNN, and SVM classifiers used in this study. Therefore, in terms of overall computational cost, our wavelet-based classification procedure would be a competitive alternative.

An important advantage of the proposed approach is that it does not require extensive data pre-processing. Feature extraction procedures proposed in previous studies rely heavily on data pre-processing. For instance, Park et al. [36], Shaban and Amara [37], and Xue et al. [38] performed WT to denoise signals observed from different bodily functions in PD diagnosis. Such pre-processing may lead to losing valuable information and negatively impact PD diagnosis performance as a result. Compared to those studies, the present study performed minimal pre-processing on VGRF time series (z-score and cumulative sum) data. This could also be a reason contributing to better classification performance.

The present study has some limitations as well. Specifically, a subset of values from the VGRF dataset was not used in the WT-based feature extraction process. In order to apply DWT, the data size has to be a power of two. In the dataset, the majority of the VGRF signals had 12,000 measurements, hence only $8,192 (= 2^{13})$ data points were used. Thus, we did not utilize approximately 4,000 measurements. In terms of time, this would amount to roughly 40 seconds of data that was not used. Although the proposed WT-based features were extracted using only 2/3's of the VGRF time series data, they distinguished gait between PD patients and controls with greater than 90% accuracy. However, the remaining 1/3 of the data may also contain valuable insights that could contribute to even greater accuracy. One possible approach to overcome this limitation is through the use of the non-decimated wavelet transform, as it is not necessary to have input signals of dyadic length.

In this study, self-similarity in VGRF data was assessed by estimating the slope of the wavelet spectra using the standard method. That is the mean of the squared wavelet coefficients was used to compute the wavelet spectra. However, the high frequency and noisy behaviors of VGRF data may hamper the ability to accurately assess self-similarity due to sensitivity of the traditional mean and variance to outliers. Other statistical measures such as median, tri-mean and distance variance can be used to assess self-similarity in a more robust way [39].

Overall, the features derived in this study are only on the basis of vertical ground reaction force. Considering ground reaction forces in other directions may also contain valuable information for better differentiation of gait between PD patients and controls.

VII. CONCLUSION

In the present study, we investigated a feature extraction procedure to identify PD based on gait data produced from PD patients and controls. A novel set of nine features was extracted on the basis of self-similarity, relationships between the left and right legs and order/disorder properties of VGRF data. These properties were characterized by performing WT on VGRF data. The set of most significant features was selected using the forward feature selection procedure, and their PD diagnosis performance was evaluated using LR, SVM, and KNN classifiers. The classifier performance was evaluated by using the multiscale feature subsets and three time domain features. The introduction of time domain features increased the classifier performance. The SVM classifier achieved the highest performance with a $97.43 \pm 2.93\%$, sensitivity 0.94 ± 0.02, and 0.99 ± 0.06 specificity. This is followed by the KNN and LR classifiers. Compared to previously published approaches, our proposed prediction methodology, which combines multiscale and time domain features, exhibits superior performance while using fewer features. This suggests that the proposed diagnostic method, which leverages multiscale (wavelet) features, can have a significant impact on improving the efficacy of PD diagnosis in a clinical setting. Therefore, outcomes of this study suggest that WT-based feature extraction procedures integrated with time domain features can serve as an effective tool in PD diagnosis.

In the spirit of reproducible research, the software used in this paper is available at https://github.com/vimalajeewaruh/Parkinson

APPENDIX A
DISCRETE WAVELET TRANSFORM (DWT)

Suppose Y represents a VGRF time series of length N, $Y = (y(t_1), y(t_2), \cdots, y(t_N))'$ at equally spaced time points t_i for $i = 1, 2, \cdots, N$. Wavelet transform of Y is given by

$$d = WY, \tag{1}$$

where d is a vector of size $N \times 1$ and W is an orthogonal matrix of size $N \times N$ of which elements are determined by wavelet filters such as Haar, Daubechies, or Symmlet.

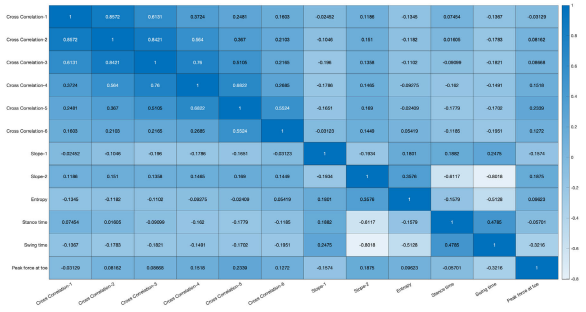

FIGURE 5. Correlation between wavelet and time domain features.

The computational complexity of WT increases with large N when matrix form-based DWT is performed. Mallat developed a computationally fast algorithm, overcoming this issue. Technical details about this algorithm can be found in Mallat [40]. The DWT on the signal Y using this algorithm results in a multiresolution representation of the signal that includes a smooth approximation ($\underset{\sim}{c}$) and hierarchy of details coefficients d_{jk} at different resolutions (scale index) j and locations k within the same resolution level. That is, the vector d given in Eq 1 contains both the discrete scaling coefficients and detail coefficients, and has the following structure

$$d = (\underset{\sim}{c}_{J_0}, \underset{\sim}{d}_{J_0}, \cdots, \underset{\sim}{d}_{J-2}, \underset{\sim}{d}_{J-1}), \tag{2}$$

where $\underset{\sim}{c}_{J_0}$ is a vector of coefficients corresponding to the smooth trend in signal Y and $\underset{\sim}{d}_j$ are details coefficients at resolution levels j such that $J_0 \leq j \leq J-1$. The coarsest decomposition level is denoted by J_0 and $J = \log_2 N$.

APPENDIX B
WAVELET SPECTRA

Consider the DWT of signal Y given in Eq 2. Suppose $\underset{\sim}{d}_j = \{d_1, d_2, \cdots, d_n\}$ represents the detail wavelet coefficients in j^{th} decomposition level. Since the wavelet coefficients have theoretically zero mean, the wavelet spectra of signal Y is computed as follows

$$S(j) = \log_2(\hat{\sigma}^2(\underset{\sim}{d}_j)), \qquad \text{for} \quad J_0 \leq j \leq J-1, \tag{3}$$

where $\hat{\sigma}^2(\underset{\sim}{d}_j)$ is an estimator for sample variance of vector $\underset{\sim}{d}_j$. The spectral slope (and Hurst exponent) is estimated from the linear regression on pairs $(j, S(j))$.

APPENDIX C
LEVEL-WISE CROSS CORRELATION COEFFICIENTS

Suppose X and Y are two VGRF time series of size $N \times 1$, and correspond to a same location in left and right leg, respectively. Also, consider that they have zero mean and finite variance (i.e., $\mathbb{E}(X) = \mathbb{E}(Y) = 0$ and $Var(X) < \infty$ and $Var(Y) < \infty$).

According to Eq 1, the DWTs on X and Y can be expressed as $d_X = WX$ and $d_Y = WY$, respectively, where W is an orthogonal matrix of size $N \times N$. The sample covariance between X and Y, $\widehat{Cov}(X, Y)$ is equivalent to the

inner-product of the DWT of X and Y. That is, $\widehat{Cov}(X, Y)$ can be computed by using Eq 2 as follows:

$$\widehat{Cov}(X, Y) = \langle d_X, d_Y \rangle = c_X^{(0)} c_Y^{(0)} + \sum_{i=1}^{J-1} \langle d_X^{(j)}, d_Y^{(j)} \rangle, \quad (4)$$

where $\langle ., . \rangle$ denotes the standard inner product in $\mathcal{R}^N$ and $\langle d_X^{(j)}, d_Y^{(j)} \rangle = \sum_{i=0}^{2^j-1} d_{j,i}^{(X)} d_{j,i}^{(Y)}$ for $j = 0, 1, \cdots, J-1$.

Eq 4 implies that the sample correlation between the signals X and Y can be expressed as the summation of level-wise inner products of their detail wavelet coefficients. Then, this leads to deriving the sample correlation coefficient between X and Y as:

$$\hat{\rho}_{X,Y} = \frac{c_X^{(0)} c_Y^{(0)}}{||d_X^{(j)}||_2 \quad ||d_Y^{(j)}||_2} + \sum_{j=0}^{J-1} w_j \hat{\rho}_{X,Y}^{(j)}, \quad (5)$$

$$\hat{\rho}_{X,Y}^{(j)} = \frac{\langle d_X^{(j)}, d_Y^{(j)} \rangle}{||d_X^{(j)}||_2 \quad ||d_Y^{(j)}||_2}, \quad \text{for} \quad 0, 1, 2, \cdots, J-1, \quad (6)$$

where $w_j = \sqrt{w_X^{(j)} w_Y^{(j)}}$, $w_X^{(j)} = \frac{||d_X^{(j)}||_2^2}{||d_X||_2}$, and $w_Y^{(j)} = \frac{||d_Y^{(j)}||_2^2}{||d_Y||_2}$. Here, $d_X^{(j)}$ and $d_Y^{(j)}$ represent the detail wavelet coefficients of X and Y at the jth scale, and $\hat{\rho}_{X,Y}^{(j)}$ is the correlation coefficient between X and Y at the j^{th} scale.

APPENDIX D
WAVELET ENTROPY

Suppose wavelet decomposition of a signal Y size $N \times 1$ and $\underset{\sim}{d}_j = \{d_1, d_2, \cdots, d_n\}$ represents the set of detail wavelet coefficients at the resolution level j. Then, non-normalized Shannon wavelet entropy (WE) of Y at jth scale level can be expressed as:

$$WE(j) = -\sum_{i=1}^{n} d_i^2 \log d_i^2. \quad (7)$$

APPENDIX E
INTERACTION BETWEEN WAVELET- AND TIME DOMAIN FEATURES

Figure 5 shows the correlation structure of the features used to build classifiers. The majority of WT-based and time domain (biomechanical) features do not share strong correlations. However, the time domain features swing time and stance time are strongly correlated with the WT-based feature slope-2, which characterizes the regularity in gait dynamics. The swing time is the time interval during which the foot is off the ground and the stance time is the time interval during which the food is on the ground while walking, and regularity in gait dynamics refers to the consistency of gait patterns. Research has shown that a decrease in regularity of gait dynamics is associated with an increase in variability in swing and stance time, which indicates instability in walking patterns [41], [42], [43]. In other words, when gait dynamics become more irregular, there is a corresponding increase in the variability of swing time. This relationship has been observed in various populations, including older adults and individuals with neurological disorders, including Parkinson's disease.

REFERENCES

[1] T. H. Hamza et al., "Genome-wide gene-environment study identifies glutamate receptor gene GRIN2A as a Parkinson's disease modifier gene via interaction with coffee," *PLOS Genet.*, vol. 7, pp. 1–15, Aug. 2011.

[2] P. Mazzoni, B. Shabbott, and J. C. Cortés, "Motor control abnormalities in Parkinson's disease," *Cold Spring Harbor Perspect. Med.*, vol. 2, no. 6, p. a009282, 2012.

[3] D. L. Murman, "Early treatment of Parkinson's disease: Opportunities for managed care," *Amer. J. Managed Care*, vol. 18, no. 7, p. S183, 2012.

[4] M. J. Armstrong and M. S. Okun, "Diagnosis and treatment of Parkinson disease: A review," *Jama*, vol. 323, no. 6, pp. 548–560, Feb. 2020.

[5] G. S. Babu and S. Suresh, "Parkinson's disease prediction using gene expression—A projection based learning meta-cognitive neural classifier approach," *Expert Syst. Appl.*, vol. 40, no. 5, pp. 1519–1529, Apr. 2013.

[6] C.-W. Lin, T.-C. Wen, and F. Setiawan, "Evaluation of vertical ground reaction forces pattern visualization in neurodegenerative diseases identification using deep learning and recurrence plot image feature extraction," *Sensors*, vol. 20, no. 14, p. 3857, Jul. 2020.

[7] T. Zhang, P. Jiang, Y. Zhang, and Y. Cao, "Parkinson's disease diagnosis based on local statistics of speech signal in time-frequency domain," *Biomed. Signal Process. Control*, vol. 38, no. 1, pp. 21–29, 2021.

[8] L. Ali, C. Zhu, Z. Zhang, and Y. Liu, "Automated detection of Parkinson's disease based on multiple types of sustained phonations using linear discriminant analysis and genetically optimized neural network," *IEEE J. Transl. Eng. Health Med.*, vol. 7, pp. 1–10, 2019.

[9] M. Murugappan, W. Alshuaib, A. K. Bourisly, S. K. Khare, S. Sruthi, and V. Bajaj, "Tunable Q wavelet transform based emotion classification in Parkinson's disease using electroencephalography," *PLoS ONE*, vol. 15, pp. 1–17, Nov. 2020.

[10] H. Mughal, A. R. Javed, M. Rizwan, A. S. Almadhor, and N. Kryvinska, "Parkinson's disease management via wearable sensors: A systematic review," *IEEE Access*, vol. 10, pp. 35219–35237, 2022.

[11] M. N. Alam, A. Garg, T. T. K. Munia, R. Fazel-Rezai, and K. Tavakolian, "Vertical ground reaction force marker for Parkinson's disease," *PLoS ONE*, vol. 12, no. 5, pp. 1–13, May 2017.

[12] G. Yogev, N. Giladi, C. Peretz, S. Springer, E. S. Simon, and J. M. Hausdorff, "Dual tasking, gait rhythmicity, and Parkinson's disease: Which aspects of gait are attention demanding?" *Eur. J. Neurosci.*, vol. 22, no. 5, pp. 1248–1256, Sep. 2005.

[13] S.-H. Lee and J. S. Lim, "Parkinson's disease classification using gait characteristics and wavelet-based feature extraction," *Expert Syst. Appl.*, vol. 39, no. 8, pp. 7338–7344, 2012.

[14] B. Su, R. Song, L. Y. Guo, and C. W. Yen, "Characterizing gait asymmetry via frequency sub-band components of the ground reaction force," *Biomed. Signal Process. Control*, vol. 18, pp. 56–60, Apr. 2015.

[15] B. Vidakovic, *Statistical Modeling by Wavelets*. Hoboken, NJ, USA: Wiley, 1999.

[16] A. Channa, R. Ceylan, and A. Baqai, "Machine learning for analyzing gait in Parkinson's patients using wearable force sensors," in *Intelligent Technologies and Applications*. Singapore: Springer, 2019, pp. 548–559.

[17] A. Aldroubi and M. Unser, *Wavelets in Medicine and Biology*. New York, NY, USA: Taylor & Francis, 1996.

[18] D. Vimalajeewa, S. A. Bruce, and B. Vidakovic, "Early detection of ovarian cancer by wavelet analysis of protein mass spectra," 2022, *arXiv:2207.07028*.

[19] S. Jeon, O. Nicolis, and B. Vidakovic, "Mammogram diagnostics via 2-D complex wavelet-based self-similarity measures," *São Paulo J. Math. Sci.*, vol. 8, no. 2, pp. 265–284, 2014.

[20] J. M. Hausdorff, J. Lowenthal, T. Herman, L. Gruendlinger, C. Peretz, and N. Giladi, "Rhythmic auditory stimulation modulates gait variability in Parkinson's disease," *Eur. J. Neurosci.*, vol. 26, no. 8, pp. 2369–2375, Oct. 2007.

[21] S. Frenkel-Toledo, N. Giladi, C. Peretz, T. Herman, L. Gruendlinger, and J. M. Hausdorff, "Effect of gait speed on gait rhythmicity in Parkinson's disease: Variability of stride time and swing time respond differently," *J. Neuroeng. Rehabil.*, vol. 2, no. 1, pp. 1–7, Dec. 2005.

[22] J. Hausdorff. (2008). *Gait in Parkinson's Disease*. Accessed: May 24, 2022. [Online]. Available: https://physionet.org/content/gaitpdb/1.0.0/

[23] Infotronic.nl. (2023). *Ultraflex Computer Dyno Graphy*. Accessed: Feb. 13, 2023. [Online]. Available: http://www.infotronic.nl/caf/

[24] F. Soares, P. Andruszkiewic, M. Freire, P. Cruz, and M. Pereira, "Self-similarity analysis applied to 2D breast cancer imaging," in *Proc. 2nd Int. Conf. Syst. Netw. Commun. (ICSNC)*, Aug. 2007, p. 77.

[25] O. A. Rosso et al., "Wavelet entropy: A new tool for analysis of short duration brain electrical signals," *J. Neurosci. Methods*, vol. 105, no. 1, pp. 65–75, Jan. 2001.

[26] S. D. Puthankattil and P. K. Joseph, "Analysis of EEG signals using wavelet entropy and approximate entropy: A case study on depression patients," *Int. J. Bioeng. Life Sci.*, vol. 8, no. 7, pp. 430–434, 2014.

[27] M. F. del Olmo and J. Cudeiro, "Temporal variability of gait in Parkinson disease: Effectsof a rehabilitation programme based on rhythmic sound cues," *Parkinsonism Rel. Disorders*, vol. 11, no. 1, pp. 25–33, Jan. 2005.

[28] S. Frenkel-Toledo, N. Giladi, C. Peretz, T. Herman, L. Gruendlinger, and J. M. Hausdorff, "Effect of gait speed on gait rhythmicity in Parkinson's disease: Variability of stride time and swing time respond differently," *J. Neuroeng. Rehabil.*, vol. 2, no. 1, p. 23, Dec. 2005.

[29] S. Frenkel-Toledo, N. Giladi, C. Peretz, T. Herman, L. Gruendlinger, and J. M. Hausdorff, "Treadmill walking as an external pacemaker to improve gait rhythm and stability in Parkinson's disease," *Movement Disorders, Off. J. Movement Disorder Soc.*, vol. 20, no. 9, pp. 1109–1114, Sep. 2005.

[30] S. Veeraragavan, A. A. Gopalai, D. Gouwanda, and S. A. Ahmad, "Parkinson's disease diagnosis and severity assessment using ground reaction forces and neural networks," *Frontiers Physiol.*, vol. 11, 2020, Art. no. 587057.

[31] H. D. Kim et al., "Analysis of vertical ground reaction force variables using foot scans in hemiplegic patients," *Ann. Rehabil. Med.*, vol. 39, no. 3, pp. 409–415, 2015.

[32] J. Yanci and J. Camara, "Bilateral and unilateral vertical ground reaction forces and leg asymmetries in soccer players," *Biol. Sport*, vol. 33, no. 2, pp. 179–183, Mar. 2016.

[33] MathWorks. (2023). *Sequentialfs*. Accessed: Feb. 13, 2023. [Online]. Available: https://www.mathworks.com/help/stats/sequentialfs.html

[34] *MATLAB, Version 9.10.0.1739362 (R2021a)*, MathWorks, Natick, MA, USA, 2021.

[35] I. El Maachi, G.-A. Bilodeau, and W. Bouachir, "Deep 1D-convnet for accurate Parkinson disease detection and severity prediction from gait," *Expert Syst. Appl.*, vol. 143, Apr. 2020, Art. no. 113075.

[36] K. H. Park et al., "Clinical outcome prediction from analysis of microelectrode recordings using deep learning in subthalamic deep brain stimulation for Parkinson's disease," *PLoS ONE*, vol. 16, pp. 1–15, Jan. 2021.

[37] M. Shaban and A. W. Amara, "Resting-state electroencephalography based deep-learning for the detection of Parkinson's disease," *PLoS ONE*, vol. 17, no. 2, pp. 1–23, 2022.

[38] Z. Xue, T. Zhang, and L. Lin, "Progress prediction of Parkinson's disease based on graph wavelet transform and attention weighted random forest," *Expert Syst. Appl.*, vol. 203, Oct. 2022, Art. no. 117483.

[39] C. Feng, Y. Mei, and B. Vidakovic, "Wavelet-based robust estimation of Hurst exponent with application in visual impairment classification," *J. Data Sci.*, vol. 18, no. 4, pp. 581–605, Jan. 2021.

[40] S. Mallat, *A Wavelet Tour of Signal Processing: The Sparse Way*. New York, NY, USA: Academic, 1999.

[41] J. M. Hausdorff and C.-K. Peng, "Multiscaled randomness: A possible source of 1/*f* noise in biology," *Phys. Rev. E, Stat. Phys. Plasmas Fluids Relat. Interdiscip. Top.*, vol. 54, no. 2, pp. 2154–2157, Aug. 1996.

[42] A. L. Goldberger, L. A. Amaral, J. M. Hausdorff, P. C. Ivanov, C. K. Peng, and H. E. Stanley, "Fractal dynamics in physiology: Alterations with disease and aging," *Proc. Nat. Acad. Sci. USA*, vol. 99, no. 1, pp. 2466–2472, 2002.

[43] J. B. Dingwell and J. P. Cusumano, "Nonlinear time series analysis of normal and pathological human walking," *Chaos, Interdiscipl. J. Nonlinear Sci.*, vol. 10, no. 4, pp. 848–863, 2000.